INTERNATIONAL JOURNAL FOR NUMERICAL METHODS IN FLUIDS, VOL. 16, 697–723 (1993)

ADAPTIVE METHODS OF LINES FOR ONE-DIMENSIONAL REACTION–DIFFUSION EQUATIONS

J. I. RAMOS

Department of Mechanical Engineering, Carnegie Mellon University, Pittsburgh, Pennsylvania 15213–3890, U.S.A. and F. Informática/E.T.S.I. Telecommunicación, Universidad de Málaga, Plaza El Ejido, s/n, 29013-Málaga, Spain

SUMMARY

Adaptive and non-adaptive finite difference methods are used to study one-dimensional reaction–diffusion equations whose solutions are characterized by the presence of steep, fast-moving flame fronts. Three non-adaptive techniques based on the methods of lines are described. The first technique uses a finite volume method and yields a system of non-linear, first-order, ordinary differential equations in time. The second technique uses time linearization, discretizes the time derivatives and yields a linear, second-order, ordinary differential equation in space, which is solved by means of three-point, fourth-order accurate, compact differences. The third technique takes advantage of the disparity in the time scales of the reaction and diffusion processes, splits the reaction–diffusion operator into a sequence of reaction and diffusion operators and solves the diffusion operator by means of either a finite volume method or a three-point, fourth-order accurate compact difference expression. The non-adaptive methods of lines presented in this paper may use equally or non-equally spaced fixed grids and require a large number of grid points to solve accurately one-dimensional problems characterized by the presence of steep, fast-moving fronts. Three adaptive methods for the solution of reaction–diffusion equations are considered. The first adaptive technique is static and uses a subequidistribution principle to determine the grid points, avoid mesh tangling and node overtaking and obtain smooth grids. The second adaptive technique is dynamic, uses an equidistribution principle with spatial and temporal smoothing and yields a system of first-order, non-linear, ordinary differential equations for the grid point motion. The third adaptive technique is hybrid, combines some features of static and dynamic methods, and uses a predictor–corrector strategy to predict the grid and solve for the dependent variables, respectively. The three adaptive techniques presented in this paper use physical co-ordinates and may employ finite volume or three-point, compact methods. The adaptive and non-adaptive finite difference methods presented in the paper are used to study a decomposition chemical reaction characterized by a scalar, one-dimensional reaction–diffusion equation, the propagation of a one-dimensional, confined, laminar flame in Cartesian co-ordinates and the Dwyer–Sanders model of one-dimensional flame propagation. It is shown that the adaptive moving method presented in this paper requires a smaller number of grid points than adaptive static, adaptive hybrid and non-adaptive methods. The adaptive hybrid method requires a smaller time step than adaptive static techniques, due to the lag between the grid prediction and the solution of the dependent variables. Non-adaptive methods of lines may yield temperature oscillations in front of and behind the flame front if Crank–Nicolson techniques are used to evaluate the time derivatives. Fourth-order accurate methods of lines in space yield larger temperature oscillations than second-order accurate methods of lines, and the magnitude of these oscillations decreases as the time step is decreased. It is also shown that three-point, fourth-order accurate discretizations of the spatial derivatives require the same number of grid points as second-order accurate, finite volume methods, in order to resolve accurately the structure of steep, fast-moving flame fronts.

KEY WORDS Methods of lines Combustion Reaction–diffusion equations Hermitian-operator methods Adaptive methods

0271–2091/93/080697–27$18.50

Received May 1992
Revised November 1992

1. INTRODUCTION

Many models of heat transfer, combustion theory, biology and epidemology are governed by one-dimensional reaction–diffusion equations whose solutions are characterized by the presence of the steep, fast-moving fronts.[1] For example, the propagation of one-dimensional laminar flames through premixed, confined or unconfined mixtures is characterized by a moving or stationary, thin flame front, where most of the chemical reactions occurs.

In order to resolve accurately the structure of steep, fast-moving fronts, one may employ adaptive or non-adaptive finite difference[1] and finite element[2] methods. Non-adaptive numerical methods employ fixed grids, which must be refined sufficiently so as to resolve the flame front structure. Since the front may move with time, a sufficiently large number of grid points must be placed throughout the entire computational domain. This means that regions far away from the flame front, where slow changes are expected, must have the same grid point density as those near the flame. As a consequence, non-adaptive numerical techniques require the solution of a large number of algebraic equations.

Adaptive techniques employ 'smart' grids whose points are concentrated near the steep, fast-moving front. Three types of adaptive methods have been developed in recent years: static, moving or dynamic, and hybrid techniques.

Adaptive static methods, also called rezoning techniques, may be based on the equidistribution of a positive weight function, the magnitude of truncation errors, variational formulations, modified equation methods, *a priori* and/or *a posteriori* error estimates, gradients of the dependent variables, etc.[2]

Adaptive moving methods may be based on equidistribution, transformation or variational principles, whereas adaptive hybrid methods[3,4] are intermediate between adaptive static techniques, where the grid points may remain fixed for intervals of time, and adaptive dynamic methods, where the grid motion is coupled fully to the solution of the partial differential equations.

In this paper, three non-adaptive and three adaptive finite difference methods of lines are presented. The first non-adaptive method uses a conservative finite volume formulation and yields a system of first-order, non-linear, ordinary differential equations in time for the values of the dependent variables, is second-order accurate in space and involves three grid points.

The second non-adaptive method of lines uses time linearization, discretizes the time derivatives and yields a system of linear, second-order, ordinary differential equations in space. This system of equations can be discretized by means of second- or fourth-order accurate spatial approximations.

We use three-point, compact finite differences to solve the system of linear, second-order, ordinary differential equations in space, which results from the time linearization of the reaction–diffusion operator.

The third non-adaptive method of lines takes advantage of the disparity in the time scales of the reaction and diffusion processes and splits the reaction–diffusion operator into a sequence of reaction and diffusion operators.[4] The reaction operator is governed by a non-linear, first-order, ordinary differential equation in time, which can be solved by means of a Newton method, whereas the diffusion operator can be solved by means of second- or fourth-order accurate methods of lines.

The three adaptive methods considered are based on the equidistribution of a positive weight function which corresponds to the arc length of the (non-dimensional) dependent variables and avoids mesh tangling and node overtaking. The first adaptive technique also uses a subequidistribution principle to ensure smooth grids and requires interpolation between the old and the new grid.

The second adaptive technique uses temporal and spatial grid smoothing and yields a system of first-order, ordinary differential equations for the grid motion. This system is fully coupled and must be solved with the partial differential equations which govern the dependent variables.

The third adaptive method considered is a hybrid technique based on a predictor–corrector procedure, which is used to predict the grid point locations and the values of the dependent variables.

The three adaptive techniques presented in this paper do not use co-ordinate transformations or Lagrangian co-ordinates. Therefore, the governing equations can be solved in the physical domain by means of the non-adaptive methods of lines presented in Section 3.

2. FORMULATION

In this paper we shall be concerned with the numerical solution of one-dimensional reaction–diffusion equations such as those which govern heat transfer phenomena with internal heat generation, biology, epidemiology, laminar flame propagation, etc. For the sake of generality, we will consider the following one-dimensional reaction–diffusion equation:

$$\frac{\partial \mathbf{U}}{\partial t} = \frac{\partial \mathbf{F}}{\partial x} + \mathbf{S}, \tag{1}$$

where t is time; x is the spatial co-ordinate; $\mathbf{U}$, $\mathbf{F}$ and $\mathbf{S}$ are N-dimensional real vectors; $\mathbf{U}$ is the vector of dependent variables; $\mathbf{S}=\mathbf{S}(\mathbf{U})$ is a non-linear source term; and

$$\mathbf{F} = \mathbf{D}\frac{\partial \mathbf{U}}{\partial x}, \tag{2}$$

where $\mathbf{D}=\mathbf{D}(\mathbf{U})$ is an $N \times N$ real diagonal matrix.

Initial and boundary conditions must be specified in order to solve equation (1) and will be given in Section 5 for the different types of problems considered in that section. For confined-flame propagation problems, the spatial co-ordinate, x, is bounded, whereas x is unbounded for unconfined-flame propagation phenomena. Furthermore, in many problems of combustion theory and biology, the solution of equation (1) is characterized by the presence of steep, fast-moving fronts which must be resolved accurately. This means that the grid used to discretize equation (1) must be sufficiently refined near and must move with the steep, fast-moving fronts.

In this paper we consider non-adaptive and adaptive finite difference methods for the discretization of equation (1). Non-adaptive methods may employ equally or non-equally spaced fixed grids and are of great importance for unconfined-flame propagation problems characterized by the presence of a stationary flame near a burner. Adaptive methods employ grids which adapt to the solution of equation (1). Such an adaption can be static, dynamic or hybrid. In static or rezoning methods, the grid is adapted in a static manner according to variational, equidistribution, and other criteria, whereas moving techniques account for the grid motion and concentrate the grid points near steep moving fronts. Hybrid techniques are intermediate between static and moving methods.

3. NON-ADAPTIVE METHODS

In this section we consider three non-adaptive methods of lines for the numerical solution of equation (1). The first method discretizes the space variable and keeps the time variable continuous, while the second technique discretizes the time variable and uses three-point, compact or Hermitian operators to solve the resulting time-discretized form of equation (1). The

third method takes advantage of disparity in the time scales of the reaction and diffusion processes.

3.1. Method of lines in time

Consider a non-equally spaced grid in x, integrate equation (1) from $x_{j-1/2}$ to $x_{j+1/2}$, where $x_{j-1/2}=(x_{j-1}+x_j)/2$, and assume that both $\mathbf{U}$ and $\mathbf{S}$ are constant within this interval of integration. The result of this integration can be written as

$$\frac{\partial \mathbf{U}_j}{\partial t}=\frac{(\mathbf{F}_{j+1/2}-\mathbf{F}_{j-1/2})}{(x_{j+1/2}-x_{j-1/2})}+\mathbf{S}_j, \tag{3}$$

where, for example,

$$\mathbf{F}_{j+1/2}=\mathbf{D}_{j+1/2}\frac{(\mathbf{U}_{j+1}-\mathbf{U}_j)}{(x_{j+1}-x_j)} \tag{4}$$

and $\mathbf{D}_{j+1/2}$ can be evaluated as

$$\mathbf{D}_{j+1/2}=[\mathbf{D}(\mathbf{U}_j)+\mathbf{D}(\mathbf{U}_{j+1})]/2 \tag{5}$$

or

$$\mathbf{D}_{j+1/2}=\mathbf{D}(\mathbf{U}_{j+1/2})=\mathbf{D}[(\mathbf{U}_j+\mathbf{U}_{j+1})/2]. \tag{6}$$

Substitution of equations (4) and (5) or (4) and (6) into equation (3) yields a system of first-order, non-linear, ordinary differential equations for $\mathbf{U}_j$. This system can be written as

$$\frac{\partial \mathbf{U}_j}{\partial t}=\mathbf{f}(\mathbf{U}_{j-1}, \mathbf{U}_j, \mathbf{U}_{j+1}), \tag{7}$$

where $\mathbf{f}(\mathbf{U}_{j-1}, \mathbf{U}_j, \mathbf{U}_{j+1})$ denotes a vector function that depends on $\mathbf{U}_{j-1}$, $\mathbf{U}_j$ and $\mathbf{U}_{j+1}$.

Equation (7) implies that the solution $\mathbf{U}_j$ at grid point x_j depends on those at its adjacent points. Furthermore, if equation (7) is to be solved at NJ grid points, the number of ordinary differential equations to be solved is $N \times NJ$, and the spatial accuracy of equation (7) is $O(\Delta x^2)$, where Δx denotes the largest value of $(x_{j+1}-x_j)$.

Equation (7) can be also written as

$$\frac{\partial \mathbf{V}}{\partial t}=\mathbf{g}(\mathbf{V}), \tag{8}$$

where $\mathbf{g}(\mathbf{V})$ denotes a vector function of $\mathbf{V}$,

$$\mathbf{V}=(\mathbf{U}_1^{\mathrm{T}}, \mathbf{U}_2^{\mathrm{T}}, \ldots, \mathbf{U}_{NJ}^{\mathrm{T}})^{\mathrm{T}}, \tag{9}$$

the superscript T denotes transpose, and the subscript $j=1, 2, \ldots, NJ$ denotes the grid points at which equation (7) is to be solved. Equation (8) can be solved by means of a variety of ordinary differential equations integrators. Note that equations (7) and (8) are, in general, stiff because of the non-linear source $\mathbf{S}$, and that, if explicit methods were used to solve equation (8), the time step would be controlled by the eigenvalue of $\partial \mathbf{g}/\partial \mathbf{V}$ whose absolute value or magnitude is the largest.

Equation (8) can be discretized by means of the following method:

$$\mathbf{V}^{n+1}-\mathbf{V}^n=\Delta t[(1-\theta)\mathbf{g}(\mathbf{V}^n)+\theta \mathbf{g}(\mathbf{V}^{n+1})], \tag{10}$$

where Δt is the time step, $\mathbf{V}^n=\mathbf{V}(t^n)$, $t^n=n\Delta t$, where n is an integer, and θ, $0 \leq \theta \leq 1$, is an implicitness parameter: the values of $\theta=0$, 1/2 and 1 denote the Euler forward, Crank–Nicolson

and the Euler backward difference methods, respectively, which are $O(\Delta t)$, $O(\Delta t^2)$ and $O(\Delta t)$ accurate, respectively.

As stated in previous paragraphs, explicit methods [$\theta=0$ in equation (10)] require small time steps and were not used in the calculations presented in this paper.

Since $\theta=1/2$ and $\theta=1$ yield implicit equations, equation (10) was solved by means of a Newton–Raphson method as follows. Equation (10) can be written as

$$\mathbf{G}(\mathbf{V}^{n+1})=\mathbf{P}(\mathbf{V}^n), \tag{11}$$

where

$$\mathbf{G}(\mathbf{V}^{n+1})=\Delta t\,\theta\mathbf{g}(\mathbf{V}^{n+1})-\mathbf{V}^{n+1}, \tag{12}$$

$$\mathbf{P}(\mathbf{V}^n)=-\mathbf{V}^n-\Delta t(1-\theta)\mathbf{g}(\mathbf{V}^n) \tag{13}$$

and $\mathbf{G}$ is a non-linear function of $\mathbf{V}$.

Equation (11) can be quasilinearized as

$$\mathbf{G}(\mathbf{V}^k)+\left(\frac{\partial\mathbf{G}}{\partial\mathbf{V}}\right)^k(\mathbf{V}^{k+1}-\mathbf{V}^k)+\text{h.o.t.}=\mathbf{P}(\mathbf{V}^n), \tag{14}$$

where the superscript k denotes the kth iteraction within the time step, h.o.t. denotes higher-order terms, and $(\partial\mathbf{G}/\partial\mathbf{V})^k=\mathbf{J}$ denotes the Jacobian matrix. Equation (14) can also be written as

$$\mathbf{V}^{k+1}=\mathbf{V}^k+\mathbf{J}^{-1}[\mathbf{P}(\mathbf{V}^n)-\mathbf{G}(\mathbf{V}^k)], \tag{15}$$

which requires the inverse of the Jacobian matrix, whose dimensions are $(N\times NJ)\times(N\times NJ)$.

In general, the computation of $\mathbf{J}^{-1}$ at each iteration and at each time step is a time-consuming task, especially if $N\times NJ$ is a large number. For this reason, the following modified, damped Newtonian method was used in the calculations:

$$\mathbf{V}^{k+1}=\mathbf{V}^k+\alpha^k\mathbf{J}^{-1}[\mathbf{P}(\mathbf{V}^n)-\mathbf{G}(\mathbf{V}^k)], \tag{16}$$

where α^k, $0<\alpha^k\leq 1$, is a damping parameter ($\alpha=1$ corresponds to the standard Newton–Raphson method) and the inverse of the Jacobian matrix, $\mathbf{J}^{-1}$, was evaluated periodically according to the following error control strategy. If the difference $|\Delta\mathbf{V}^k|=|\mathbf{V}^{k+1}-\mathbf{V}^k|$ within the time step is larger than 1% of $\mathbf{V}^k$, the Jacobian matrix was re-evaluated, i.e. the Jacobian matrix was not re-evaluated unless $|\Delta\mathbf{V}^k|$ was larger than $0{\cdot}01\mathbf{V}^k$. Note that, in combustion problems, the temperature and species mass fractions are greater than or equal to zero, i.e. $\mathbf{V}\geq 0$,

Substantial computer savings were also obtained by storing the LU-decomposition of $\mathbf{J}$. Note that $\mathbf{J}$ can be decomposed as

$$\mathbf{J}=\mathbf{LU}, \tag{17}$$

where $\mathbf{L}$ and $\mathbf{U}$ are lower and upper tridiagonal matrices, respectively.

The convergence rate of the Newtonian method given by equation (15) is quadratic, provided that the initial estimate of $\mathbf{V}$ is close enough to the solution. In the calculations presented in this paper, the initial guess for the solution of equation (16) always was $\mathbf{V}^n$, i.e. the value of $\mathbf{V}$ at the previous time step, and the iterative, modified, damped Newton technique was stopped and the time was advanced when the following convergence criterion was satisfied:

$$[(\Delta\mathbf{V}^k)^{\mathrm{T}}\cdot\Delta\mathbf{V}^k]^{1/2}=\sum_{i=1}^{NJ}[(\Delta\mathbf{V}_i^k)^{\mathrm{T}}\cdot\Delta\mathbf{V}_i^k]^{1/2}\leq 10^{-5}. \tag{18}$$

Equation (18) corresponds to the L_2-norm of the vector $\Delta\mathbf{V}^k$.

3.2. Method of lines in space

In the method of lines considered in the previous section, space was discretized and the time variable was kept continuous. In this section, we consider methods of lines based on the discretization of the time variable.

Consider equation (1), which can be discretized in time as

$$\frac{\Delta \mathbf{U}}{\Delta t}=(1-\theta)\mathbf{Q}^n+\theta\mathbf{Q}^{n+1}, \tag{19}$$

where $\Delta\mathbf{U}=\mathbf{U}^{n+1}-\mathbf{U}^n$, θ, $0\leq\theta\leq 1$, is an implicitness parameter and

$$\mathbf{Q}=\frac{\partial \mathbf{F}}{\partial x}+\mathbf{S}. \tag{20}$$

For the same reasons as those stated in the previous section, we will consider only the Euler backward and Crank–Nicolson methods corresponding to $\theta=1$ and $\theta=1/2$, respectively.

Equation (19) can be linearized with respect to time as follows:

$$\mathbf{Q}^{n+1}=\mathbf{Q}^n+\left(\frac{\partial \mathbf{Q}}{\partial \mathbf{t}}\right)^n \Delta t+\mathrm{O}(\Delta t^2) \tag{21}$$

and, since t and x are independent variables, $\mathbf{S}$ is only a function of $\mathbf{U}$, and $\mathbf{F}$ is a function of $\mathbf{U}$ and $\partial\mathbf{U}/\partial x$,

$$\mathbf{S}^{n+1}=\mathbf{S}^n+\left(\frac{\partial \mathbf{S}}{\partial \mathbf{U}}\right)^n \Delta\mathbf{U}+\mathrm{O}(\Delta t^2), \tag{22}$$

$$\mathbf{F}^{n+1}=\mathbf{F}^n+\left(\frac{\partial \mathbf{F}}{\partial \mathbf{U}}\right)^n \Delta\mathbf{U}+\left(\frac{\partial \mathbf{F}}{\partial \mathbf{U}_x}\right)^n \Delta\mathbf{U}_x+\mathrm{O}(\Delta t^2), \tag{23}$$

where $\mathbf{U}_x=\partial\mathbf{U}/\partial x$.

Substitution of equations (21)–(23) into equation (19) yields

$$\frac{\Delta \mathbf{U}}{\Delta t}=\mathbf{Q}^n+\theta\left[\frac{\partial}{\partial x}(\mathbf{A}^n\Delta\mathbf{U})+\frac{\partial}{\partial x}\left(\mathbf{B}^n\frac{\partial\Delta\mathbf{U}}{\partial x}\right)+\mathbf{C}^n\Delta\mathbf{U}\right], \tag{24}$$

where

$$\mathbf{A}=\frac{\partial \mathbf{F}}{\partial \mathbf{U}}=\mathbf{U}_x^*\frac{\mathrm{d}\mathbf{D}}{\mathrm{d}\mathbf{U}}, \qquad \mathbf{B}=\frac{\partial \mathbf{F}}{\partial \mathbf{U}_x}=\mathbf{D}, \qquad \mathbf{C}=\frac{\partial \mathbf{S}}{\partial \mathbf{U}}, \tag{25}$$

$\mathbf{U}_x^*$ is an $N\times N$ diagonal matrix whose elements are the derivatives of the components of $\mathbf{U}$ with respect to x, i.e. the ith element of $\mathbf{U}_x^*$ is $\partial U_i/\partial x$, where U_i denotes the ith component of the vector $\mathbf{U}$, and $\mathrm{d}\mathbf{D}/\mathrm{d}\mathbf{U}$ is an $N\times N$ matrix whose ith row consists of the elements $\partial D_i/\partial U_j$, $j=1, 2, \ldots, N$, and D_i is the element in the ith row and column of the diagonal matrix $\mathbf{D}$. Note that $\mathbf{A}$, $\mathbf{B}$ and $\mathbf{C}$ are functions of space and time because they depend on $\mathbf{U}$, which is a function of t and x.

The spatial derivatives in equation (24) can be discretized by means of second-order, conservative, finite differences to yield a block tridiagonal matrix for the vector $\mathbf{U}$. In this paper, however, equation (24) is discretized by means of three-point, fourth-order accurate, compact or Hermitian differences, as shown in the sequel.

Equation (24) can also be written as

$$\mathbf{a}\frac{\partial^2 \mathbf{y}}{\partial x^2}+\mathbf{b}\frac{\partial \mathbf{y}}{\partial x}+\mathbf{c}\mathbf{y}=\mathbf{d}, \tag{26}$$

where

$$y=\Delta\mathbf{U}, \qquad \mathbf{a}=\theta\mathbf{B}^n, \qquad \mathbf{b}=\theta\left(\frac{\partial\mathbf{B}^n}{\partial x}+\mathbf{A}^n\right), \tag{27}$$

$$\mathbf{c}=\theta\left(\frac{\partial\mathbf{A}^n}{\partial x}+\mathbf{C}^n\right)-\frac{\mathbf{I}}{\Delta t}, \qquad \mathbf{d}=-\mathbf{Q}^n \tag{28}$$

and $\mathbf{I}$ is a unit matrix.

Equation (24) represents a linear, second-order, ordinary differential equation for $\mathbf{y}$. The linearity of this equation is a consequence of the time linearization represented by equation (21) and the fact that $\mathbf{a}$, $\mathbf{b}$, $\mathbf{c}$ and $\mathbf{d}$ are evaluated at $t^n=n\Delta t$, whereas equation (26) is to be solved for $\Delta\mathbf{U}$ or $\mathbf{U}^{n+1}$. Note that $\mathbf{a}$, $\mathbf{b}$ and $\mathbf{c}$ are $N\times N$ matrices.

The linearity of equation (26) allows us to employ three-point, compact or Hermitian difference formulae as follows.[5,6] Equation (26) can be written as

$$\mathbf{aG}+\mathbf{bW}+\mathbf{cy}=\mathbf{d}, \tag{29}$$

where $\mathbf{G}=\partial^2\mathbf{y}/\partial x^2$ and $\mathbf{W}=\partial\mathbf{y}/\partial x$.

Equation (29) can be applied at the non-equally spaced grid points x_{j-1}, x_j and x_{j+1} to obtain three equations with nine unknowns, i.e. $\mathbf{y}_{j-1}$, $\mathbf{y}_j$, $\mathbf{y}_{j+1}$, $\mathbf{W}_{j-1}$, $\mathbf{W}_j$, $\mathbf{W}_{j+1}$, $\mathbf{G}_{j-1}$, $\mathbf{G}_j$ and $\mathbf{G}_{j+1}$. Furthermore, one can use the following Taylor series expansions:

$$\mathbf{y}_{j+1}=\mathbf{y}_j+\mathbf{W}_jH+\frac{1}{2}\mathbf{G}_jH^2+\frac{1}{6}\frac{\partial^3\mathbf{y}_j}{\partial x^3}H^3+\frac{1}{24}\frac{\partial^4\mathbf{y}_j}{\partial x^4}H^4+\mathrm{O}(H^5), \tag{30}$$

$$\mathbf{y}_{j-1}=\mathbf{y}_j-\mathbf{W}_jh+\frac{1}{2}\mathbf{G}_jh^2-\frac{1}{6}\frac{\partial^3\mathbf{y}_j}{\partial x^3}h^3+\frac{1}{24}\frac{\partial^4\mathbf{y}_j}{\partial x^4}h^4+\mathrm{O}(h^5), \tag{31}$$

$$\mathbf{W}_{j+1}=\mathbf{W}_j+\mathbf{G}_jH+\frac{1}{2}\frac{\partial^3\mathbf{y}_j}{\partial x^3}H^2+\frac{1}{6}\frac{\partial^4\mathbf{y}_j}{\partial x^4}H^3+\mathrm{O}(H^4), \tag{32}$$

$$\mathbf{W}_{j-1}=\mathbf{W}_j-\mathbf{G}_jh+\frac{1}{2}\frac{\partial^3\mathbf{y}_j}{\partial x^3}h^2-\frac{1}{6}\frac{\partial^4\mathbf{y}_j}{\partial x^4}h^3+\mathrm{O}(h^4), \tag{33}$$

$$\mathbf{G}_{j+1}=\mathbf{G}_j+\frac{\partial^3\mathbf{y}_j}{\partial x^3}H+\frac{1}{2}\frac{\partial^4\mathbf{y}_j}{\partial x^4}H^2+\mathrm{O}(H^3), \tag{34}$$

$$\mathbf{G}_{j-1}=\mathbf{G}_j-\frac{\partial^3\mathbf{y}_j}{\partial x^3}h+\frac{1}{2}\frac{\partial^4\mathbf{y}_j}{\partial x^4}h^2+\mathrm{O}(h^3), \tag{35}$$

where $H=x_{j+1}-x_j$ and $h=x_j-x_{j-1}$.

From equations (34) and (35), we can obtain the values of $\partial^3\mathbf{y}_j/\partial x^3$ and $\partial^4\mathbf{y}_j/\partial x^4$ as functions of $\mathbf{G}_{j-1}$, $\mathbf{G}_j$ and $\mathbf{G}_{j+1}$. These values can then be substituted into equations (30)–(33) to obtain four algebraic equations for $\mathbf{y}_k$, $\mathbf{W}_k$ and $\mathbf{G}_k$, with $k=j-1$, j, $j+1$, i.e. four equations with nine unknowns. These four equations plus equation (29), applied at $j-1$, j and $j+1$, provide seven equations with nine unknowns, which can be used to eliminate the values of $\mathbf{W}_{j-1}$, $\mathbf{W}_j$, $\mathbf{W}_{j+1}$, $\mathbf{G}_{j-1}$, $\mathbf{G}_j$ and $\mathbf{G}_{j+1}$ and to obtain the following linear algebraic equation:[6]

$$\alpha\mathbf{y}_{j-1}+\beta\mathbf{y}_j+\chi\mathbf{y}_{j+1}=\delta, \tag{36}$$

where α, β and χ are $N\times N$ matrices, δ is an N-dimensional vector, and the values of α, β, χ and δ depend on H and h and on the values of $\mathbf{a}$, $\mathbf{b}$, $\mathbf{c}$ and $\mathbf{d}$ at the grid points $j-1$, j and $j+1$.

Boundary conditions can easily be implemented in equation (36). If boundary conditions of the third (Robin) type are specified, the system of seven equations mentioned above is applied at the

first interior point near the boundary together with the boundary conditions to obtain a system of eight equations with nine unknowns. This system can be used to eliminate the values of $\mathbf{W}_{j-1}$, $\mathbf{W}_j$, $\mathbf{W}_{j+1}$, $\mathbf{G}_{j-1}$, $\mathbf{G}_j$, $\mathbf{G}_{j+1}$ and the value of $\mathbf{y}$ two grid points away from the boundary. This elimination yields a linear equation for the value of $\mathbf{y}$ at the boundary as a function of the value of $\mathbf{y}$ at the next point closest to the boundary. This linear equation at the boundary has to be solved together with equation (36), which is valid only at interior points.

Equation (36) is a three-point, fourth-order accurate, linear algebraic equation which has a block tridiagonal structure and can be written as

$$\mathbf{MY}=\mathbf{H}, \tag{37}$$

where $\mathbf{Y}=[\mathbf{y}_1^{\mathrm{T}}, \mathbf{y}_2^{\mathrm{T}}, \ldots, \mathbf{y}_{NJ}^{\mathrm{T}}]^{\mathrm{T}}$ represents the column vector of dependent variables at the points $j=1, 2, \ldots, NJ$, where equation (36) is to be solved, $\mathbf{M}$ is an $(N\times NJ)\times(N\times NJ)$ square matrix and $\mathbf{H}$ is an $N\times NJ$ vector. $\mathbf{M}$ is a block tridiagonal matrix because α, β and χ in equation (36) depend only on the values of $\mathbf{y}$ at $j-1, j, j+1$. The matrix $\mathbf{M}$ can be written in LU-decomposition form, i.e. $\mathbf{M}=\mathbf{LU}$, and equation (37) can be written as

$$\mathbf{LY}^*=\mathbf{H}, \tag{38}$$

$$\mathbf{UY}=\mathbf{Y}^*. \tag{39}$$

Equation (38) can easily be solved by forward substitution to evaluate $\mathbf{Y}^*$, which can then be substituted into equation (39) to obtain $\mathbf{Y}$ by backward substitution.

It must be pointed out that the discretization of equation (1) presented in Section 3.1 is conservative, while that presented in this section is not, because the diffusion terms in equation (24) were differentiated in order to obtain equation (26). It must also be pointed out that equations (24) and (26) are both linear, whereas equation (8) is highly non-linear.

3.3. Operator-splitting methods of lines

The methods of lines presented in Sections 3.1 and and 3.2 can also be used with operator-splitting techniques, which take advantage of the disparity in the time scales of the diffusion and reaction processes which are present in equation (1). The characteristic diffusion and reaction times of equation (1) can be estimated as

$$t_{\mathrm{d}}=\frac{\Delta x^2}{\|\mathbf{D}\|}, \qquad t_{\mathrm{r}}=\left\|\frac{\partial \mathbf{S}}{\partial \mathbf{U}}\right\|^{-1}, \tag{40}$$

where t_{d} and t_{r} denote the characteristic diffusion and reaction times and $\|\mathbf{D}\|$ and $\|\partial\mathbf{S}/\partial\mathbf{U}\|$ represent the norms of the diagonal marix $\mathbf{D}$ and of the matrix $\partial\mathbf{S}/\partial\mathbf{U}$, respectively. For example, the values of $\|\mathbf{D}\|$ and $\|\partial\mathbf{S}/\partial\mathbf{U}\|$ may be set equal to the largest absolute value of the eigenvalues of $\mathbf{D}$ and $\partial\mathbf{S}/\partial\mathbf{U}$, respectively. If $t_{\mathrm{d}}\ll t_{\mathrm{r}}$, diffusion phenomena are slower than those associated with the source term $\mathbf{S}$. One can take advantage of the difference between t_{d} and t_{r} by splitting the reaction–diffusion operator of equation (1) into the following sequence of reaction and diffusion operators:

$$L_{\mathrm{R}}\colon \frac{\partial \mathbf{U}}{\partial t}=\mathbf{S}, \tag{41}$$

$$L_{\mathrm{D}}\colon \frac{\partial \mathbf{U}}{\partial t}=\frac{\partial \mathbf{F}}{\partial x}, \tag{42}$$

where L_{R} and L_{D} denote reaction and diffusion operators, respectively. The diffusion operator

involves spatial derivatives and can be discretized by using the same techniques as those presented in Sections 3.1 and 3.2, whereas the reaction operator represents a system of first-order, non-linear, ordinary differential equations, which can be solved by means of the Newton method presented in Section 3.1.

The diffusion operator represented by equation (42) can be solved by means of the Euler backward or Crank–Nicolson methods with a time step Δt, and, if $t_d/t_r > 1$, one can solve the reaction operator NT times, where NT is the natural number closest to t_d/t_r. Therefore, if $t_d > t_r$, equation (41) is solved NT times with a time step equal to $\Delta t/NT$ using as initial condition $\mathbf{U}^n$. The resulting value of $\mathbf{U}$, i.e. $\mathbf{U}^*$, is used as initial condition for the solution of equation (42) and the solution is said to have converged if equation (18) is satisfied. This approximation can be justified both analytically and numerically, for the condition $t_d > t_r$ implies that the chemical reactions occur at a much faster rate than the diffusion processes and since, in order to resolve accurately the chemical reaction processes, the time step must be smaller than the chemical reaction time, t_r, the diffusion processes may be assumed to be frozen in the time scale of the chemical reactions. This approximation can also be justified by means of asymptotic methods, e.g. the method of multiple scales, due to the disparity in the time scales of the reaction and diffusion processes.

The methods of lines presented in Sections 3.1 and 3.3 are iterative, whereas those of Section 3.2 are not.

4. ADAPTIVE METHODS OF LINES

The methods of lines presented in Section 3 use fixed grids which should concentrate the grid points in regions where steep gradients of the vector $\mathbf{U}$ exist. Since $\mathbf{U}$ is an N-dimensional vector, it is possible that the components of this vector exhibit steep gradients at different axial locations. If this occurs, the grid may have to be concentrated at different axial locations. In most combustion problems, however, a good criterion for grid refinement is the temperature profile, i.e. only one component of the vector $\mathbf{U}$ is sufficient to refine the grid.

In one-dimensional, laminar-flame propagation problems, the flame front may move as a function of time and the grid should be adapted or moved in such a manner that a sufficiently large number of grid points is located at the flame front so that its structure is resolved accurately.

Three different adaptive techniques can be used to refine the grid and follow steep, fast-moving fronts: static, hybrid and moving methods. In static or rezoning methods, the grid is refined, where needed, according to some criterion such as equidistribution of the arc length of the temperature profile, variational principles which minimize a functional, etc. In moving or dynamic methods, differential equations for the grid point motion are solved in conjuntion with equation (1). The equations for the grid point motion may be obtained from variational principles, equidistribution techniques, etc. A major difference between adaptive static and adaptive dynamic or moving methods is that, in static methods, the grid points may remain fixed for intervals of time, whereas, in dynamic methods, the grid motion and the finite difference form of equation (1) are fully coupled at each time step. Hybrid techniques are intermediate between static and dynamic methods.

In the next subsections, static, dynamic or moving and hybrid adaptive methods of lines are presented.

4.1. Adaptive static method of lines

Adaptive static methods of lines may be based on equidistribution principles, gradients of the dependent variables, truncation errors, Richardson's extrapolation, variational formulations,

etc.[2] In this section, we consider equidistribution techniques based on the equidistribution of a positive weight function.

Consider equation (1) and the strictly positive weight function defined by

$$w(t, x)=\left[1+\left(\frac{\partial \mathbf{U}^{\mathrm{T}}}{\partial x}\cdot\frac{\partial \mathbf{U}}{\partial x}\right)^2\right]^{1/2}=\left[1+\sum_{i=1}^{N}\left(\frac{\partial U_i}{\partial x}\right)^2\right]^{1/2}, \tag{43}$$

which represents the arc length of the N-th dimensional vector $\mathbf{U}$. Equation (43) can be discretized at the $(j-1/2)$th grid point as

$$w_j=\left\{1+\sum_{i=1}^{N}\left[\frac{(U_i)_{j+1}-(U_i)_j}{x_{j+1}-x_j}\right]^2\right\}^{1/2}. \tag{44}$$

It must be pointed out that both, the co-ordinate x and the vector $\mathbf{U}$, must be non-dimensional in equation (43), and that equation (1) should be non-dimensionalized when using equidistribution principles and weight functions.

As previously stated, the different components, U_i, of the vector $\mathbf{U}$ may exhibit steep gradients at different spatial locations. In most combustion problems, however, the temperature gradient can be used to define the weight function instead of equation (43), which accounts for the gradients of all components of $\mathbf{U}$.

Numerical solutions of two-point boundary value problems in ordinary differential equations have shown that numerical errors can be reduced by equidistributing the weight function w over all the computational domain as[7]

$$\int_{x_{j-1}}^{x_j} w(t, x)\,\mathrm{d}x=\int_{x_j}^{x_{j+1}} w(t, x)\,\mathrm{d}x. \tag{45}$$

Equation (44) can be discretized as

$$h_j w_j=h_{j+1} w_{j+1}, \tag{46}$$

where $h_j=x_j-x_{j-1}$, and w_j denotes the value of the weight function at $x_{j-1/2}$ [cf. equation (44)]. Since $w>0$, the grid points cannot cross each other, and mesh tangling and node overtaking are not possible.

Equations (44) and (46) are to be solved, together with the discretized form of equation (1) as presented in Sections 3.1 and 3.3, to determine $\mathbf{U}$ and x_j. The solution of equations (1) and (46) can be obtained iteratively. However, if a fixed number of grid points, NJ, is used in the calculations, the equidistribution principle given by equation (46) does not restrict the size of adjacent grid intervals, and equation (46) and the finite difference expression of equation (1) may yield stiff and/or ill-conditioned matrices and may require a large number of iterations to achieve convergence. In order to obtain smooth grids and/or avoid ill-conditioned matrices and long computational times, the sizes of adjacent grid spacings must be restricted in such a manner that

$$K^{-1}\leq\frac{h_{j+1}}{h_j}\leq K, \tag{47}$$

where $K\geq 1$.

In the calculations presented in this paper, $K=1{\cdot}2$, and equation (47) ensures that the grid spacing does not change substantially from one interval to the next one.

The numerical solution of the discretized form of equation (1) presented in Sections 3.1 and 3.3 and of equation (46) proceeds as follows. The initial conditions, i.e. $\mathbf{U}(0, x)$ is used in equation (46) to determine x_j; wherever equation (47) is not satisfied, grid points are added/deleted so as to satisfy both equations (46) and (47). With the grid spacing so obtained, equation (1) is solved with

any of the techniques presented in Sections 3.1 and 3.3 and a new weight function, w, is obtained, which is again used to solve equation (46) and determine x_j so that equation (47) is satisfied. This iterative procedure is repeated as many times as necessary until equation (18) is satisfied.

The locations of the grid points, x_j, may vary during the iterative procedure and from one time step to another or when grid points are added and/or deleted so as to satisfy equation (47). When this occurs, an interpolation procedure must be devised to interpolate the values of the dependent variable $\mathbf{U}^k$ determined in the grid x_j^k on the new grid x_j^{k+1}, where the superscript k denotes the kth iteration or kth time step. This interpolation must be performed in such a manner that the monotonicity, positivity and conservation properties of $\mathbf{U}$ are satisfied.

Conservation can be ensured provided that

$$\int_a^b U_i^k(t, x)\,dx = \int_a^b U_i^{k+1}(t, x)\,dx, \qquad i=1, 2, \ldots, N. \tag{48}$$

where $a \le x \le b$, $(b-a)$ denotes the length of the physical domain, and the left- and right-hand sides of equation (48) are to be evaluated in the grids x_j^k and x_j^{k+1}, respectively.

If linear interpolation is used to evaluate U_i^k and U_i^{k+1} in the grids x_j^k and x_j^{k+1}, respectively, equation (47) provides the value of U_i^{k+1} in the new grid x_j^{k+1}. This linear interpolation also ensures the positivity and monotonocity of U_i^{k+1}. In this paper, the integrals in equation (48) were evaluated by means of a second-order accurate, trapezoidal rule.

4.2. Adaptive moving method of lines

The main disadvantages of the adaptive static technique presented in Section 4.1 are that the grid point locations are determined iteratively from equations (46) and (47), and that the grid refinement is performed once the solution of equation (1) has been obtained. As a consequence, the grid points may remain fixed for intervals of time, the iterative and interpolation procedures have to be repeated every time that grid points are added and/or deleted so that equation (47) is satisfied, and there is no dynamic coupling between the equidistribution principle represented by equation (46) and the discretized form of equation (1).

In this section, an adaptive moving method of lines based on the technique developed by Dorfi and Drury[7] is presented. The starting point of this dynamic method is equations (44) and (46), which ensure that mesh tangling and node overtaking are not possible because w is strictly positive. However, regularization in both space and time is required to avoid ill-conditioned matrices, slow convergence and adjacent grid spacings of disparate sizes.

Following Dorfi and Drury,[7] we first introduce spatial smoothing as follows. The grid point concentration can be defined as

$$n_j = (x_{j+1} - x_j)^{-1}, \tag{49}$$

so that equation (46) becomes

$$\frac{n_{j-1}}{w_{j-1}} = \frac{n_j}{w_j} \tag{50}$$

and the spatial grid smoothing is performed by replacing n_j in equation (50) by the following smoothed values

$$\tilde{n}_j = n_j - k(k+1)(n_{j+1} - 2n_j + n_{j-1}), \quad k>0, \tag{51}$$

so that the location of the grid points is determined from the following equation:

$$\frac{\tilde{n}_{j-1}}{w_{j-1}}=\frac{\tilde{n}_j}{w_j}. \tag{52}$$

This smoothing procedure is equivalent to a filtering technique which ensures that

$$\frac{k}{k+1}\leq\frac{n_{j-1}}{n_j}\leq\frac{k+1}{k} \tag{53}$$

and which restricts the grid point concentration in a manner similar to equation (47).

The following boundary conditions were imposed on equation (52)

$$n_2=n_1, \qquad n_{NJ}=n_{NJ-1}, \tag{54}$$

i.e. the gradients of the grid point concentration are equal to zero at both $x=a$ and $x=b$.

Equations (51), (52) and (54) represent a system of algebraic equations which can be transformed into a system of ordinary differential equations by means of the temporal smoothing introduced in the next paragraphs.

The temporal smoothing is based on the replacement of w by

$$R=\int_0^\infty w(t-\sigma\tau)e^{-\sigma}\,d\sigma, \qquad \tau\geq 0. \tag{55}$$

Note that if $\tau\equiv 0$, then $R=w$.

Integration of equation (55) yields

$$w=R+\tau\frac{dR}{dt}. \tag{56}$$

We now assume that the grid point concentration $\tilde{n}$ is proportional to R rather than to w as shown in equation (52). If c (=constant) is the proportionality constant, $R=c\tilde{n}$ can be substituted into equation (56) to yield

$$w=c\left(\tilde{n}+\tau\frac{d\tilde{n}}{dt}\right). \tag{57}$$

Substitution of equation (57) into equation (52) yields

$$\frac{\tilde{n}_{j-1}+\tau\,d\tilde{n}_{j-1}/dt}{w_{j-1}}=\frac{\tilde{n}_j+\tau\,d\tilde{n}_j/dt}{w_j}. \tag{58}$$

It must be noted that, according to equations (56)–(58), the grid motion is prevented from adjusting immediately to the new values of w and that R forces the grid to adjust to the new values of w over a delay time interval equal to τ. This 'delayed' adjustment avoids temporal oscillations in the grid point trajectories. It must also be noted that if $\tau=0$, $w=R$ [cf. equation (56)], and an equidistribution technique [cf. equation (58)] similar to that presented in Section 4.1 is obtained. If τ is very large, the grid motion lags far behind the solution of any propagating steep front.

Equation (51) can be substituted into equation (58) to obtain an ordinary differential equation for dn_j/dt, whose value can be calculated by means of equation (49) as

$$\frac{dn_j}{dt}=-\frac{dx_{j+1}/dt-dx_j/dt}{(x_{j+1}-x_j)^2}. \tag{59}$$

Substitution of equations (49), (51) and (59) into equation (58) yields an ordinary differential for the grid motion which is subject to equation (54).

The discretized form of equation (1) presented in Section 3.1 together with the ordinary differential equation for x_j described in previous paragraphs can be written as

$$\mathbf{M}(\mathbf{V})\frac{\mathrm{d}\mathbf{V}}{\mathrm{d}t}=\mathbf{P}(\mathbf{V}), \tag{60}$$

where

$$\mathbf{V}=(\mathbf{U}_1^{\mathrm{T}}, x_1, \mathbf{U}_2^{\mathrm{T}}, x_2, \ldots, \mathbf{U}_{NJ}^{\mathrm{T}}, x_{NJ})^{\mathrm{T}} \tag{61}$$

and the subscripts $1, 2, \ldots, NJ$ denote the grid points at which $\mathbf{U}$ and x are to be evaluated. Note that, at the boundaries of the physical domain, $x=a$ and $x=b$; therefore, the co-ordinates of these points are specified, whereas the values of $\mathbf{U}(t, a)$ and $\mathbf{U}(t, b)$ have to be evaluated if Neumann or Robin boundary conditions are used. Note also that the substitution of equations (49), (51) and (59) into equation (58) yields an ordinary differential at the jth point which depends on $x_{j-2}, x_{j-1}, x_j, x_{j+1}, x_{j+2}, \mathrm{d}x_{j-2}/\mathrm{d}t, \mathrm{d}x_{j-1}/\mathrm{d}t, \mathrm{d}x_j/\mathrm{d}t, \mathrm{d}x_{j+1}/\mathrm{d}t$ and $\mathrm{d}x_{j+2}/\mathrm{d}t$, whereas equation (7) depends on $\mathbf{U}_{j-1}, \mathbf{U}_j, \mathbf{U}_{j+1}, x_{j-1}, x_j$ and x_{j+1}.

Equation (60) was solved by means of the Euler backward difference method and the modified, damped, Newton–Raphson technique presented in Section 3.1 until equation (18) was satisfied.

4.3. Adaptive hybrid method of lines

The static and dynamic methods of lines presented in Sections 4.1 and 4.2, respectively, are based on an equidistribution principle [cf. equation (45)], whose precise meaning can be interpreted as follows. Consider the mapping $(t, x)\mapsto(\xi, \eta)$, where

$$\xi=t, \qquad \eta=\frac{\int_a^x w(t, x)\,\mathrm{d}x}{\int_a^b w(t, x)\,\mathrm{d}x}, \tag{62}$$

which implies that $0\leq\eta\leq 1$.

If an equally spaced grid is used in the co-ordinate η, i.e. $\eta_j-\eta_{j-1}=\eta_{j+1}-\eta_j$, then equation (45) is obtained.

The mapping defined by equation (62) can be substituted into equation (1) to obtain

$$\frac{\partial\mathbf{U}}{\partial\xi}+\frac{\partial\mathbf{U}}{\partial\eta}\frac{\partial\eta}{\partial t}=\frac{\partial\eta}{\partial x}\frac{\partial\mathbf{F}}{\partial\eta}+\mathbf{S}, \tag{63}$$

where

$$\frac{\partial\eta}{\partial x}=\frac{w(t, x)}{\int_a^b w(t, x)\,\mathrm{d}x}. \tag{64}$$

Since $\partial\eta/\partial x=(\partial x/\partial\eta)^{-1}$ and $\partial\eta/\partial t=-(\partial\eta/\partial x)(\partial x/\partial\xi)$, equation (63) can be written as

$$\frac{\partial x}{\partial\eta}\frac{\partial\mathbf{U}}{\partial\xi}-\frac{\partial x}{\partial\xi}\frac{\partial\mathbf{U}}{\partial\eta}=\frac{\partial x}{\partial\eta}\mathbf{Q}, \tag{65}$$

where

$$\mathbf{Q}=\frac{\partial\mathbf{F}}{\partial x}+\mathbf{S}. \tag{66}$$

Equations (62) and (65) or equations (62) and (63) provide integral and partial differential equations for the grid motion $x(\tau, \eta)$ and $\mathbf{U}(\tau, \eta)$, respectively. However, if a fixed number of grid points were used in the calculations, the grid motion would adapt immediately to the value of the weight function and oscillations would be produced unless a temporal smoothing similar to that

presented in Section 4.2 is employed. In the absence of temporal and spatial smoothing [cf. equations (47) and (51)], the grid may not be smooth and the discretization of equation (65) may result in ill-conditioned matrices and/or slow convergence rates.

In this section, we present an adaptive hybrid method of lines, which is an intermediate technique between the static and dynamic methods of lines presented in Sections 4.1 and 4.2, respectively. The hybrid method of lines presented in this section is a predictor–corrector scheme, which consists of a predictor step and a corrector step. In the predictor step, it is assumed that $\partial x/\partial\xi=0$ so that equation (65) becomes

$$\frac{\partial \mathbf{U}}{\partial \xi}=\mathbf{Q}. \tag{67}$$

Equation (67) can be solved by means of the methods presented in Sections 3.1 and 3.3 to yield the value $\mathbf{U}^*$, which is then used in equation (62) to obtain the values of x_j^*. These values are then assumed to be equal to x_j^{n+1}.

In the corrector step, equation (65) is discretized as

$$[\theta(x_{j+1}^{n+1}-x_{j-1}^{n+1})+(1-\theta)(x_{j+1}^{n}-x_{j-1}^{n})]\frac{\partial \mathbf{U}_j}{\partial \xi}-[\theta(\mathbf{U}_{j+1}-\mathbf{U}_{j-1})+(1-\theta)(\mathbf{U}_{j+1}^{n}-\mathbf{U}_{j-1}^{n})]$$

$$\times\frac{x_j^{n+1}-x_j^{n}}{\Delta\xi}=\theta(x_{j+1}^{n+1}-x_{j-1}^{n+1})\mathbf{Q}_j+(1-\theta)(x_{j+1}^{n}-x_{j-1}^{n})\mathbf{Q}_j^{n}, \tag{68}$$

where $0\leq\theta\leq 1$, the spatial derivatives have been discretized, and $\partial x/\partial\xi$ has been replaced by $(x_j^*-x_j^n)/\Delta\xi=(x_j^{n+1}-x_j^n)/\Delta\xi$.

The values $\theta=1$ and $\theta=\frac{1}{2}$ correspond to the implicit and Crank–Nicolson methods, respectively, and equation (68) represents a non-linear, first-order, ordinary differential equation for $\mathbf{U}_j$ which can be solved by means of the Newton method as indicated in equation (16). In the calculations presented in this paper the value $\theta=\frac{1}{2}$ was used in equation (68), and equation (67) was solved by means of the modified, damped Newton–Raphson method presented in Section 3.1 with $\theta=1$.

The main advantage of the hybrid technique presented in this paper is that grid tangling and node overtaking are avoided because the weight function, w, is strictly positive. Another advantage is that the predictor and corrector steps, and the grid motion and the solution of equation (1) are not fully coupled at each time step. However, the technique has the following drawbacks. First, it does not ensure smooth grids because a subequidistribution principle similar to equation (47) or grid smoothing similar to equation (51) is not used. This may result in slow convergence of the Newton method. Second, the grid motion is not coupled fully to the solution of $\mathbf{U}$ and there is a lag between the predicted grid x_j^* and the solution $\mathbf{U}^{n+1}$. This lag is a consequence of the assumption that $x_j^{n+1}=x_j^*$ and may require the use of small time steps to obtain accurate solutions, especially if the solution is characterized by the presence of a steep, fast-moving front. This lag can, however, be reduced, if not eliminated, by using the solution $\mathbf{U}^{n+1}$ in equation (62) to obtain an improved value of x_j^* and by repeating this iterative procedure until the difference between the values of x_j^* in two successive iterations of the corrector step is sufficiently small. Unfortunately, this iterative procedure was found to be more time-consuming than the adapive static method of lines presented in Section 3.1 and was not used in the calculations presented in this paper where the time step was chosen to be sufficiently small so as to obtain accurate results.

The third main disadvantage of the hybrid method of lines described in this section is that Newton's method may fail to converge when determining the initial grid, i.e. the grid x_j^n based on

the known solution $\mathbf{U}^n$, if equation (46) is used. This problem was solved by using the following equation [cf. equation (64)]:

$$\frac{\partial x}{\partial \eta}=\frac{\int_a^b w(t, x)\,dx}{w(t, x)}. \tag{69}$$

Since $\mathbf{U}^n$ is known from the initial conditions, the weight function, w [cf. equation (43)], is also known, and equation (69) can be solved to obtain $x(\xi^n, \eta)$. Note that $\eta(t, a)=0$ and $\eta(t, b)=1$.

It must be pointed out that the adaptive hybrid method presented in this section may also use the subequidistribution principle of equation (47) in order to ensure smooth grids.

5. PRESENTATION OF RESULTS

In this section the non-adaptive and adaptive finite difference methods presented in Sections 3 and 4 are applied to a variety of one-dimensional problems. Some of these problems have been solved previously by the author, using finite element methods.[2]

5.1. One-step decomposition reaction

As a first application of the numerical methods presented in Sections 3 and 4, we consider a one-step decomposition reaction governed by the following non-dimensional equation and initial and boundary conditions:

$$\frac{\partial T}{\partial t}=\frac{\partial^2 T}{\partial x^2}+D(1+\alpha-T)\exp(-\delta/T), \qquad t>0, \quad 0<x<1, \tag{70}$$

$$\frac{\partial T}{\partial x}(0, t)=0, \qquad T(t, 1)=1, \qquad T(0, x)=1, \tag{71}$$

where T is the temperature, $\alpha=1$, $\delta=20$, $D=R\exp(\delta)/\alpha\delta$ and $R=5$.

Equations (70) and (71) represent a mathematical model of a one-step decomposition reaction characterized by the conversion of fuel to combustion products. It is also a one-dimensional model of heat transfer phenomena with internal heat generation, and has been analysed previously by Petzold[8] and Adjerid and Flaherty,[9] who used adaptive moving finite difference methods based on variational formulations and moving finite element methods with error control, respectively. The adaptive finite difference technique employed by Petzold[8] was based on the minimization of the time rate of change of $\mathbf{U}$ and x in the co-ordinates (τ, η) and this minimization yielded an equation for the grid velocity. In order to avoid mesh tangling and grid point collisions, Petzold[8] used a penalty formulation which gives adjacent points nearly equal velocities.

Adjerid and Flaherty[9] used a finite element method with linear test and trial functions and spatial error estimates to move the grid and refine it locally so as to equidistribute a measure of the total spatial error.

Equation (70) was solved by means of the non-adaptive and adaptive finite difference methods presented in Sections 3 and 4. Thirty-six grid points were used with the adapive dynamic method presented in Section 4.2 as compared to the thirty and twenty grid points employed by Petzold[8] and Adjerid and Flaherty,[9] respectively.

Figures 1 and 2 show the temperature profiles and the locations of some of the grid points as functions of time. In particular, Figure 1 shows the ignition of the fuel and the flame propagation at selected times. The temperature profiles shown in Figure 1 are in very good agreement with those of Petzold[8] and Adjerid and Flaherty.[9]

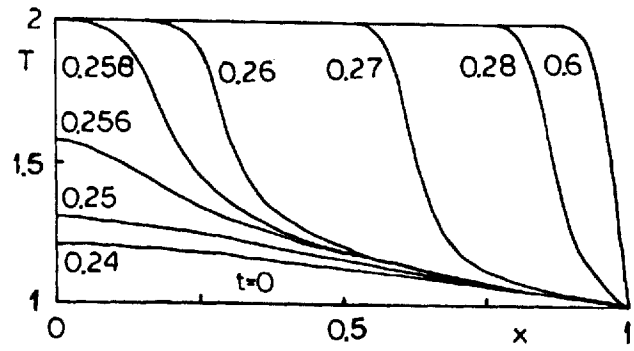

Figure 1. Temperature profiles

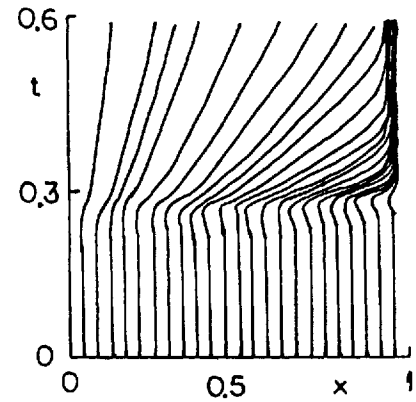

Figure 2. Locations of the grid points

Petzold[8] showed that the ignition time and the temperatre profiles are very sensitive to the number of grid points and to the adaptive moving method used in the calculations. This is due to the extremely fast rate of ignition, the flame front velocity, and the exponential non-linearity of the source term in equation (70). A similar behaviour was also observed in the computations performed with the adaptive moving method of lines presented in Section 4.2. As indicated in Section 4.2, if the delay time, τ, in equation (58) is too large, the grid motion lags far behind the solution of the steep, moving flame front.

Adjerid and Flaherty[9] also showed that the ignition time and the computed temperature profiles are very sensitive to the value of the parameter which controls the difference between the velocities of two adjacent nodes. For small values of that parameter, the grid motion is too slow and unable to follow the flame front. On the other hand, large values of that parameter result in grids which are able to follow the rapidly moving flame front but concentrate the grid points near $x=0$, where ignition takes places, and the computations require small time steps.

Furzeland *et al.*[10] solved equation (70) by means of finite difference methods based on the adaptive techniques proposed by Dorfi and Drury[7] and Petzold.[8] They also used the moving finite element method developed by Miller,[11] performed numerical studies aimed at assessing the reliability, robustness and efficiency of these three adaptive techniques and recommended the method proposed by Dorfi and Drury over those of Petzold and Miller based on the numerical solution of equation (70), the viscous Burgers equation, and two advection–reaction–diffusion

equations whose solutions are characterized by waves travelling in opposite directions. Furzeland *et al.*[10] also showed that Petzold' method is reliable and robust, but it requires interpolation and many evaluations of the Jacobian matrix.

The numerical results shown in Figure 2 indicate that the solution is characterized by two different processes; initially, an ignition kernel is formed near $x=0$, whereas at later times, a flame front propagates toward the right boundary. These two proceses are characterized by two different time scales. The formation of the ignition kernel proceeds at a faster rate than the flame propagation. Therefore, small time steps must be taken in order to simulate ignition accurately. If the time step is large, any errors in the numerical simulation of ignition will affect the flame propagation at later times.

The adaptive moving method presented in Section 4.2 was solved with 36 grid points and $\tau=10^{-8}$. The time step was varied from 10^{-6} at ignition, i.e. when the mixture is ignited at $x=0$, to 10^{-4}, when a propagating flame front was established. The number of evaluations of the Jacobian matrix depended on the time step used in the calculations and on τ. In particular, small values of τ required small number of evaluations of the Jacobian matrix: the values of $\tau=10^{-6}$ and $\tau=10^{-8}$ required 874 and 268 evaluations, respectively, of the Jacobian matrix in the Newton method when the time step was set equal to 10^{-5} throughout the calculations. For a time step equal to 10^{-4}, the values of $\tau=10^{-6}$ and $\tau=10^{-8}$ required 5031 and 1354 evaluations of the Jacobian matrix, respectively. The differences in the number of evaluations of the Jacobian matrix were due to the extremely fast ignition rate and the number of grid points used in the calculations. For $\tau=10^{-8}$ and a time step equal to 10^{-5}, calculations with 25 grid points required 893 evaluations of the Jacobian matrix as compared to 268 evaluations for 36 grid points and the same values of the time step and the delay time.

Equations (70) and (71) were also solved with the adaptive static and adaptive hybrid methods presented in Sections 4.1 and 4.3, respectively. The adaptive static method of Section 4.1 was initialized with 100 grid points and required 739 evaluations of the Jacobian matrix. The same method required 1671 evaluations of the Jacobian matrix when 50 grid points were used in the calculations. In both cases, the time step had to be equal to 10^{-6} in order to satisfy the convergence criterion of equation (18) and avoid a higher number of evaluations of the Jacobian matrix.

The adaptive hybrid method of Section 4.3 was also initialized with 100 grid points and required 1083 evaluations of the Jacobian matrix when a time step equal to 10^{-5} was employed in the calculations. In order to keep the total number of evaluations of the Jacobian matrix below 800, it was found that the time step should never be greater than 10^{-5}. Otherwise, the Newton method would require more iterations to satisfy the convergence criterion of equation (18) and/or the accuracy of the adaptive hybrid method would be extremely poor. This is due to the fast ignition rate, the high velocity of the moving flame front, and the exponential non-linearity of the non-linear source term in equation (70). Note that in the adaptive hybrid method of Section 4.3, the predictor step is used to predict a grid which does not correspond to the solution of equations (70) and (71), i.e. there is a lag between the predicted grid and the solution of the corrector step. This lag increases as the time step is increased, especially if the problem under study involves a fast-moving front such as the one shown in Figure 1.

It was also observed that the convergence rate of the adaptive hybrid method of Section 4.3 can be improved if equation (47) is used so as to ensure smooth grids. However, the adaptive hybrid method with equation (47) always required a larger number of evaluations of the Jacobian matrix than the adaptive static method of Section 4.1 when the same number of grid points was used in both techniques. This was also attributed to the lag between the predictor step which is used to calculate the grid, and the corrector step which is used to evaluate the temperature.

Both the adaptive static and the adaptive hybrid methods always required more than 50 grid points to keep the total number of evaluations of the Jacobian matrix below 800. Note that the adaptive moving method required fewer than 268 evaluations of the Jacobian matrix and used bigger time steps than the adaptive static and the adaptive hybrid methods.

Equations (70) and (71) were also solved with the non-adaptive methods of lines presented in Sections 3.1–3.3. It was found that the Crank–Nicolson methods ($\theta=\frac{1}{2}$) of Section 3 required a slightly higher number of evaluations of the Jacobian matrix than the Euler backward or implicit ($\theta=1$) technique.

The method of lines of Section 3.1 employed equally spaced grids with 250 grid points to achieve the same accuracy as the adaptive moving method of Section 4. The fourth-order accurate method of lines presented in Section 3.2 also required the same number of grid points to obtain an accurate resolution of the steep moving flame front. A smaller number of grid points yielded temporal oscillations in front of and behind the flame, and the size of these oscillations could be reduced only by either decreasing the grid spacing and/or the time step used in the calculations. Therefore, although the method of lines of Section 3.2 has more spatial accuracy than that of Section 3.1, the accurate resolution of steep moving flame fronts requires that both techniques employ nearly the same number of grid points. Furthermore, the fourth-order accurate method of lines of Section 3.2 required smaller time steps than that of Section 3.1, because of the linearization of the source term [cf. equation (22)]. Note that equation (36) is linear; therefore, the accuracy of the solution depends on the time step used in the calculations. On the other hand, equation (10) is non-linear and must be solved iteratively until equation (18) is satisfied.

The second- and fourth-order accurate methods of lines presented in Sections 3.1 and 3.2, respectively, were used to solve the diffusion operator of equation (42), whereas the reaction operator of equation (41) was solved by means of the Newtonian method. Since equation (70) is a scalar equation with a diffusion coefficient equal to one, the characteristic diffusion time [cf. equation (40)] is Δx^2, whereas the characteristic reaction time is a function of space, because the source term is a function of space. The characteristic reaction time employed to solve equation (41) corresponded to the largest temperature.

The method of lines of Section 3.2 was found to be less accurate than that of Section 3.1 for the solution of the diffusion operator [cf. equation (42)]. This result is consistent with those obtained by the author in his numerical studies of one-dimensional scalar equations.[5] Note that the methods of lines of Sections 3.1–3.3 used the same number of grid points, i.e. 250, and that the accuracy of operator-splitting methods deteriorates at a higher rate than those of Sections 3.1 and 3.2 as the time step and/or grid spacing are increased due to the partial uncoupling between the reaction and diffusion operators of equations (41) and (42), respectively.

5.2. *Confined-flame propagation*

Consider a one-dimensional laminar flame in Cartesian co-ordinates and assume that the Soret and Dufour effects, pressure gradient diffusion, body forces, bulk viscosity and radiative heat transfer are negligible. Assume also that the Mach number is small, so that the pressure is spatially uniform and that the chemical species diffuse according to Fick's law with equal diffusion coefficients and that the species' specific heats at constant pressure are equal and constant. Under these assumptions, the equations governing the flame propagation can be written as

$$\frac{\partial \rho}{\partial t^*}+\frac{\partial}{\partial z}(\rho u)=0, \tag{72}$$

$$p=p(t^*), \tag{73}$$

$$\frac{\partial(\rho Y_i)}{\partial t^*}+\frac{\partial}{\partial z}(\rho u Y_i)=\frac{\partial}{\partial z}\left(\rho D\frac{\partial Y_i}{\partial z}\right)+\dot{\omega}_i, \qquad i=1, 2, \ldots, NS, \tag{74}$$

$$\rho C_p\left(\frac{\partial T}{\partial t^*}+u\frac{\partial T}{\partial z}\right)=\frac{\mathrm{d}p}{\mathrm{d}t}+\frac{\partial}{\partial z}\left(\lambda\frac{\partial T}{\partial z}\right)-\sum_{i=1}^{NS} h_i^0\dot{\omega}_i, \tag{75}$$

$$p=\rho\tilde{R}T\sum_{i=1}^{NS}\frac{Y_i}{M_i}, \tag{76}$$

$$\sum_{i=1}^{NS} Y_i=1, \tag{77}$$

where t^* is time, z is the Cartesian co-ordinate, ρ, p and T denote the mixture density, pressure and temperature, respectively, u is the mixture velocity, D and λ are the diffusion coefficient and heat conductivity, respectively, Y_i, $\dot{\omega}_i$ and h_i^0 denote the mass fraction, reaction rate and enthalpy of formation of species i, respectively, NS is the number of chemical species, $\tilde{R}$ is the universal gas constant and M_i denotes the molar mass of species i. Equations (72)–(75) represent the continuity, linear momentum, species and energy conservation equations, respectively. Equation (76) is the equation of state for the mixture, which was assumed to be composed of ideal gases.

Equations (72)–(75) are to be solved for $t>0$ and $0<z<L$, and represent a mixed system of advection–reaction–diffusion equations which can be transformed into a system of reaction–diffusion equations by means of the von Mises transformation,

$$(t^*, z)\rightarrow(t, x), \tag{78}$$

where

$$t=t^*, \qquad M\frac{\partial x}{\partial z}=\rho, \qquad M\frac{\partial x}{\partial t^*}=-\rho u, \tag{79}$$

$$M=\int_0^L \rho\,\mathrm{d}z, \tag{80}$$

and M denotes the mass per unit area.

Substitution of equations (78) and (79) into equations (72), (74) and (75) yields

$$\frac{\partial u}{\partial x}=M\frac{\partial}{\partial t}\left(\frac{1}{\rho}\right), \tag{81}$$

$$\frac{\partial Y_i}{\partial t}=\alpha\frac{\partial^2 Y_i}{\partial x^2}+\frac{\dot{\omega}_i}{\rho}, \qquad i=1, 2, \ldots, NS, \tag{82}$$

$$\frac{\partial T}{\partial t}=\frac{1}{\rho C_p}\left(\frac{\mathrm{d}p}{\mathrm{d}t}-\sum_{i=1}^{NS} h_i^0\dot{\omega}_i\right)+\alpha\frac{\partial^2 T}{\partial x^2}, \tag{83}$$

where $\alpha=\rho^2 D/M^2$ has been assumed to be constant and the Lewis number, $Le=\lambda/\rho C_p D$, was assumed to be equal to one. The value of $\mathrm{d}p/\mathrm{d}t$ in equation (83) can be calculated as follows. Due to the low Mach number assumption, the pressure is spatially uniform [cf. equation (73)], and equation (76) can be integrated from $z=0$ to $z=L$ to yield

$$p=\frac{\tilde{R}}{L}\int_0^L \rho T\sum_{i=1}^{NS}\left(\frac{Y_i}{M_i}\right)\mathrm{d}z=\frac{M\tilde{R}}{L}\int_0^1 T\sum_{i=1}^{NS}\left(\frac{Y_i}{M_i}\right)\mathrm{d}x, \tag{84}$$

where equation (79) has been used.

Equations (82)–(84) are of the integrodifferential reaction–diffusion type and can be integrated from $x=0$ to $x=1$ by means of the non-adaptive and adaptive finite difference methods presented in Sections 3 and 4, respectively. Once Y_i ($i=1, 2, \ldots, NS$) and T are known, equations (84) and (76) can be used to calculate $p(t)$ and $\rho(t, x)$, and integration of equation (81) yields the fluid velocity. Note that $u(t, 0)=u(t, L)=0$.

The Cartesian co-ordinate z can be calculated from equation (79) as

$$z=M\int_0^x \frac{\mathrm{d}x}{\rho}. \tag{85}$$

In the calculations presented in this section, the following one-step irreversible chemical reaction was considered:

$$C_3H_8+5O_2\rightarrow 3CO_2+4H_2O \tag{86}$$

$$\dot{\omega}_1=-M_1\Omega, \qquad \dot{\omega}_2=-5M_2\Omega, \tag{87}$$

$$\dot{\omega}_3=3M_3\Omega, \qquad \dot{\omega}_4=4M_4\Omega, \tag{88}$$

$$\Omega=K\exp\left(-\frac{E}{\tilde{R}T}\right)\rho^2\frac{Y_1}{M_1}\frac{Y_2}{M_2}, \tag{89}$$

where subscripts 1–4 denote propane, oxygen, carbon dioxide and water vapour, respectively; $M_1=M_3=44$ g, $M_2=32$ g, $M_4=18$ g, $E=30\,000$ cal/mol is the activation energy of the reaction, $K=1{\cdot}27\times10^{13}$ cm^3/·, $\alpha=2{\cdot}17\times10^{-7}$ s^{-1}, $C_p=7$ cal/mol/K, $L=10$ cm, $NS=4$ and

$$\sum_{i=1}^{NS} h_i^0\dot{\omega}_i=Q\dot{\omega}_1, \tag{90}$$

where $Q=11\,070$ cal/g denotes the heat of combustion. Equations (72)–(73) and equations (81) and (83), with $p=$constant, govern the propagation of one-dimensional low Mach number, unconfined, laminar flames. In fact, equation (70) represents a simplified non-dimensional model of equations (82) and (83).

Equation (84) can be substituted into equation (83) and the resulting equation together with equation (82) can be solved, by means of the methods of lines presented in Sections 3 and 4, subject to the following boundary conditions:

$$\frac{\partial T}{\partial x}(t, 0)=\frac{\partial T}{\partial x}(t, L)=0, \tag{91}$$

$$\frac{\partial Y_i}{\partial x}(t, 0)=\frac{\partial Y_i}{\partial x}(t, L)=0. \tag{92}$$

It must be noted that the co-ordinate x in equation (79) is non-dimensional and that equations (82) and (83) were first written in non-dimensional form as follows. The initial temperature and pressure, and α^{-1} were used in the non-dimensionalization of T, p and t, respectively. The reason for this non-dimensionalization is that the adaptive methods of lines presented in Section 4 use a weight function which depends on the gradients of the dependent variables. Note that the species mass fractions are dimensionless.

The initial conditions used to solve equations (82)–(84) corresponded to a stoichiometric mixture and are illustrated in Figures 3 and 4, which show the dimensional temperature (T) and the fuel mass fraction (Y_1) profiles at different times. These initial conditions correspond to the presence of burnt mixture at the left boundary and were imposed so as to avoid the time-

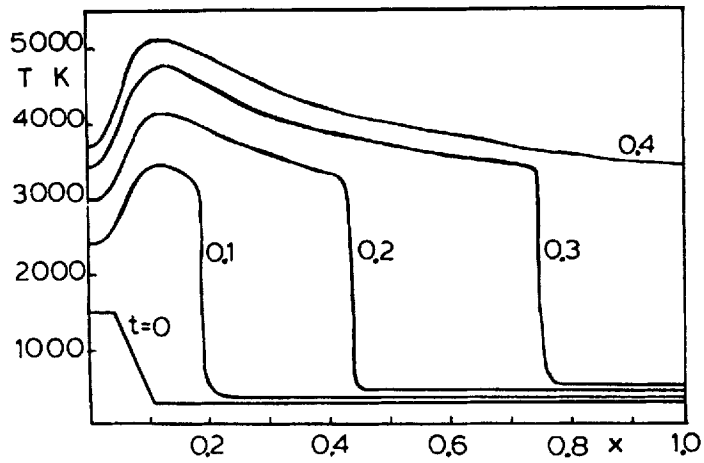

Figure 3. Temperature profiles

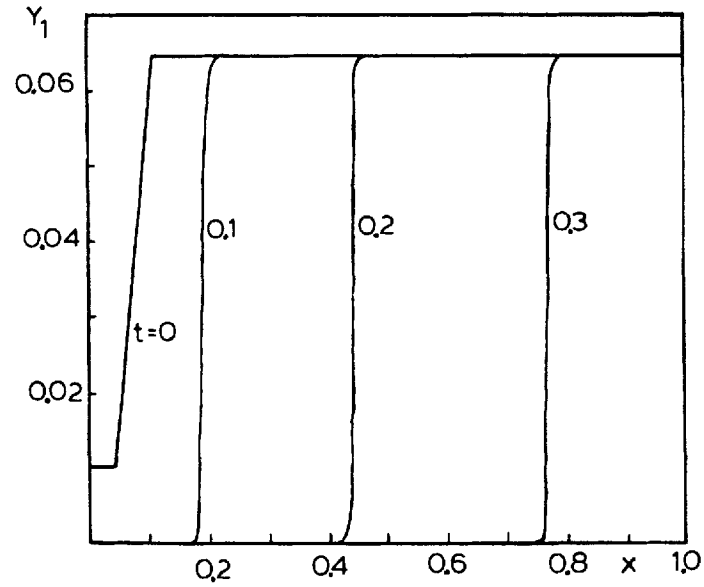

Figure 4. Propane mass fraction profiles

consuming simulation of ignition at that boundry. Note that ignition was simulated in Section 5.1.

The results shown in Figures 3 and 4 were obtained by means of the adaptive moving method presented in Section 4.2 with 50 grid points, $\tau = 10^{-7}$ and a variable time step. The value of τ used in this section is higher than that used in Section 5.1, where ignition was simulated, and the time step was varied in such a manner so as to keep the number of the evaluations of the Jacobian matrix below 250. The adaptive moving method of Section 4.2 used the method of lines of Section 3.1 with $\theta = 1$.

Equations (82)–(84) were also solved with the adaptive static and adaptive hybrid finite difference methods of Sections 4.1 and 4.3, respectively. The adaptive static method required between 67 and 93 grid points and a time step of 10^{-7} in order to satisfy the convergence criterion of equation (18) and keep the number of evaluations of the Jacobian matrix below 250. Larger time steps and/or fewer grid points resulted in a slower convergence rate of the Newton method and a larger number of evaluations of the Jacobian matrix. The slow convergence rate was attributed to the frequent need for regridding required to satisfy equation (47). Note that since a confined flame is considered, the mixture temperature and pressure increase with time; therefore, the magnitude of the non-linear source terms and the flame speed also increase with time.

The adaptive hybrid method of Section 4.3 also required between 67 and 93 grid points to satisfy the convergence criterion of equation (18) and keep the number of evaluations of the Jacobian matrix below 250. However, the hybrid method required the use of a time step equal to 10^{-8} and the use of equation (47). If equation (47) were not used, the grid would not be smooth and a larger number of iterations would be required to satisfy equation (18) if $\Delta t = 10^{-8}$. Moreover, if equation (47) is used, but $\Delta t > 10^{-8}$, the number of evaluations of the Jacobian matrix also increases because of the lag between the grid predicted in the predictor step and the solution corresponding to the corrector step. Note that the temperature and the fuel mass fraction profiles steepen and the flame speed increases with time due to the confinement of the mixture (cf. Figures 3 and 4). Therefore, in order to avoid a large lag between the predictor and corrector steps, the time step had to be reduced, as indicated in previous paragraphs.

In order to obtain as accurate results as those of the adaptive moving method of Section 4.2, the non-adaptive techniques presented in Section 3 required 1600 grid points. The method of lines of Section 3.1 employed a time step equal to 10^{-6} and yielded oscillations in front of and behind the flame front if $\theta = \frac{1}{2}$. The magnitude of these oscillations was reduced by decreasing the time step. No oscillations were observed for $\theta = 1$ and $\Delta t = 10^{-6}$.

The fourth-order accurate method of lines with $\theta = 1$ required a $\Delta t = 10^{-7}$ to achieve the same accuracy as the adaptive moving technique of Section 4.2. The difference in time steps between the methods of lines of Sections 3.1 and 3.2 is due to the time linearization of the source terms in Section 3.2.

The fourth-order accurate method of lines with $\theta = \frac{1}{2}$ and $\Delta t = 10^{-7}$ yielded temperature oscillations in front of and behind the flame front. The magnitude of these oscillations was higher than that of the methods of lines of Section 3.1, with $\theta = \frac{1}{2}$ and $\Delta t = 10^{-7}$, and could be reduced by decreasing the time step. Similar oscillations were observed when the methods of lines of Sections 3.1 and 3.2, with $\theta = \frac{1}{2}$, were used to solve the diffusion operator of Section 3.3.

The operator-splitting methods of Section 3.3 yielded slightly slower flame fronts than those predicted by the numerical techniques of Sections 3.1 and 3.2. The solution of the diffusion operator by means of the fourth-order accurate method of lines presented in Section 3.2 yielded a slower flame than that predicted by the numerical technique presented in Section 3.1 for $\Delta t = 10^{-7}$. However, the accuracy of the operator-splitting technique increases as the time step is decreased.

The large difference in the number of grid points used by the non-adaptive and adaptive methods presented in Sections 3 and 4, respectively, to solve the flame propagation problems of Sections 5.1 and 5.2, is due to the simulation of ignition in Section 5.1 and the flame front thickness in Section 5.2. The numerical simulation of ignition in Section 5.1 requires the use of small time steps in order to resolve accurately the formation of the ignition kernel near $x = 0$; however, the thickness of the flame front presented in Section 5.1 is much larger and its resolution requires fewer grid points than that of Section 5.2.

5.3. The Dwyer–Sanders model of one-dimensional laminar-flame propagation

The Dwyer–Sanders model of one-dimensional laminar-flame propagation can be obtained from equations (82) and (83) by assuming that the pressure is constant. The resulting set of non-dimensional equations can be written as[12]

$$\frac{\partial Y}{\partial t}=\frac{\partial^2 Y}{\partial x^2}-Y\Omega(T), \qquad t>0, \quad 0<x<1, \tag{93}$$

$$\frac{\partial T}{\partial t}=\frac{\partial^2 T}{\partial x^2}+Y\Omega(T), \qquad t>0, \quad 0<x<1, \tag{94}$$

where

$$\Omega(T)=3{\cdot}52\times 10^{-6}\exp\left(-\frac{4}{T}\right). \tag{95}$$

Equations (93)–(95) are subject to the following initial and boundary conditions:

$$Y(0, x)=1, \qquad T(0, x)=0{\cdot}2, \tag{96}$$

$$\frac{\partial Y}{\partial x}(t, 0)=\frac{\partial T}{\partial x}(t, 0)=0, \tag{97}$$

$$\frac{\partial Y}{\partial x}(t, 1)=0, \tag{98}$$

$$T(t, 1)=\begin{cases} 0{\cdot}2+t/0{\cdot}0002, & 0<t<0{\cdot}0002, \\ 1{\cdot}2, & t\geq 0{\cdot}0002. \end{cases} \tag{99}$$

Equations (93)–(99) correspond to the ignition of a confined, one-dimensional mixture where the right-boundary temperature is increased linearly with time until it reaches a value equal to 1·2.

Equations (93) and (94) were solved by means of the adaptive moving method of Section 4.2, with $\tau=10^{-8}$, $\Delta t=10^{-6}$ and 25 grid points, and the results of this method are illustrated in Figures 5–7, which show the temperature and fuel mass fraction profiles and the locations of some of the grid points, respectively, at selected times.

Figures 5 and 6 show the ignition of the fuel at $x=0$ and the fast propagation of a steep moving flame front towards the left boundary, located at $x=0$, whereas Figure 7 shows that the grid follows and concentrates the points at the flame front.

Petzold[8] and Verwer *et al.*[3] have also solved equations (93)–(99) by means of adaptive moving methods. In particular, Petzold[8] used an adaptive technique which minimizes the time rate of change of $\mathbf{U}$ and x, and yields a first-order, ordinary differential equation in time for the grid motion.

Verwer *et al.*[3] used an adaptive hybrid, space–time finite element technique similar to the hybrid method of lines presented in Section 4.3 and showed that iterative techniques may not converge when determining the initial grid. Verwer *et al.*[3] also expanded the finite element discretizations of equations (92) and (93) around the old grid in order to obtain the partial differential equations represented truly by the finite element method.[13,14] The resulting modified equation contains second-order derivatives with respect to time and mixed derivatives with respect to space and time, and can be used to control the time step by controlling the magnitude of the temporal truncation errors. Note that the spatial discretization errors are somewhat controlled by the equidistribution technique [cf. equation (62)]; however, in adaptive methods,

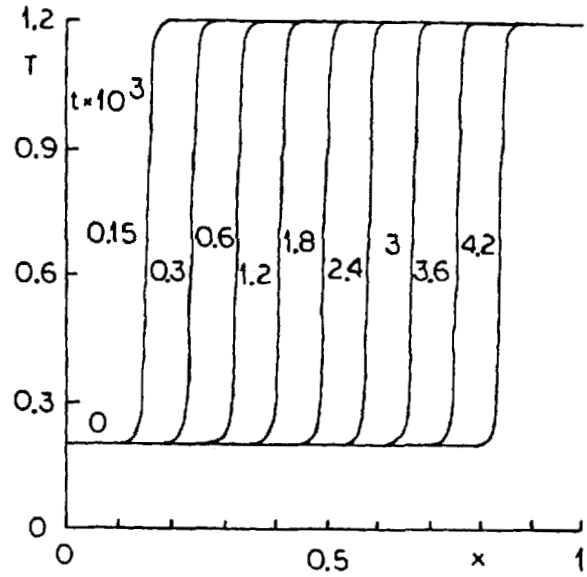

Figure 5. Temperature profiles

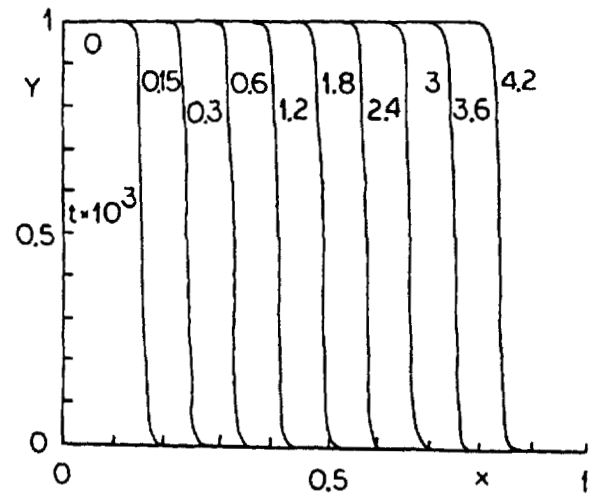

Figure 6. Fuel mass fraction profiles

both space and time are coupled through the grid motion, and the spatial and temporal truncation errors are necessarily related.

The adaptive moving method of Section 4.2, with $\Delta t = 10^{-6}$, $\tau = 10^{-8}$ and 25 grid points, required 132 evaluations of the Jacobian matrix in the Newton method. This number increased as τ was increased; for example, $\tau = 10^{-6}$ and $\tau = 10^{-7}$ required 257 and 168 evaluations of the Jacobian matrix, respectively.

Equations (92) and (93) were also solved with the adaptive static and adaptive hybrid methods of Sections 4.1 and 4.3. The adaptive static method employed 64 grid points and $\Delta t = 10^{-6}$ to achieve the same accuracy as the adaptive moving technique and required 147 evaluations of the

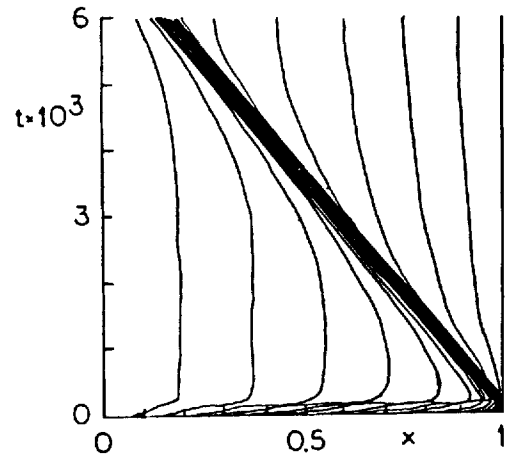

Figure 7. Locations of the grid points

Jacobian matrix. For $\Delta t = 10^{-6}$ and 45 grid points, the adaptive method of Section 4.1 required 451 evaluations of the Jacobian matrix; most of these evaluations were due to interpolation and regridding and can be reduced by using smaller time steps.

The adaptive hybrid method of Section 4.3 also used 64 grid points and a time step equal to 10^{-7} and required 201 evaluations of the Jacobian matrix. The smaller time step used by the adaptive hybrid method is a consequence of the lag between the predictor and corrector steps. Larger time steps yielded oscillatory temperature profiles in front of and behind the flame front due to the uncoupling between the predicted grid and the solution of the partial differential equations. Note that equations (92) and (93) are characterized by the presence of a steep, fast-moving flame front as illustrated in Figures 5 and 6.

Equations (92) and (93) were also solved in equally spaced grids by means of the non-adaptive methods presented in Sections 3.1–3.3. These methods required 1200 grid points to achieve the same accuracy as the adaptive moving method of Section 4.2. The method of lines of Section 3.1 used a time step of 10^{-6}, whereas that of Section 3.2 employed a $\Delta t = 5 \times 10^{-7}$ because of the linearization of the non-linear reaction–diffusion operator and the high speed of the moving flame front. Larger time steps deteriorated the accuracy of the time linearization procedure used in Section 3.2 and yielded oscillatory temperature profiles in front of and behind the steep flame front. In some cases, these oscillations yielded negative species mass fractions.

The operator-splitting techniques of Section 3.3 required time steps equal to 10^{-6} and 5×10^{-7} when the methods of lines of Sections 3.1 and 3.2, respectively, were used to solve the diffusion operator. Larger time steps resulted in a larger number of evaluations of the Jacobian matrix and temperature oscillations, specially if $\theta = \frac{1}{2}$ was used in the methods presented in Sections 3.1–3.3.

6. CONCLUSIONS

Three non-adaptive and three adaptive methods of lines have been used to study three one-dimensional, laminar-flame propagation problems. The first non-adaptive technique uses a finite volume formulation to discretize the spatial co-ordinate and yields a system of first-order, non-linear, ordinary differential equations in time, which was solved by means of a modified, damped Newton method. The second non-adaptive method uses time linearization, discretizes

the time derivatives and yields a system of second-order, linear, ordinary differential equations, which was solved by means of three-point, compact, finite differences.

The third non-adaptive technique takes advantage of the disparity in the time scales of the reaction and diffusion processes, splits the reaction–diffusion operator into a sequence of reaction and diffusion operators, and solves the reaction operator by means of a modified, damped Newton method. The diffusion operator was solved by means of second- and fourth-order accurate methods of lines.

The three adaptive methods of lines presented in this paper are based on the equidistribution of the arc length of the vector of the dependent variables. The first adaptive technique is static and uses a subequidistribution principle to avoid non-smooth grids. The second adaptive technique is dynamic, uses temporal and spatial smoothing procedures and yields a system of non-linear, ordinary differential equations for the grid motion, which is solved iteratively together with the discretized forms of the partial differential equations for the dependent variables.

The third adaptive method is an intermediate technique based on a predictor–corrector procedure where the predictor step is used to predict the grid point locations, whereas the corrector step is employed to determine the dependent variables.

Application of the three adaptive methods presented in this paper to three one-dimensional, laminar-flame propagation problems indicates that adaptive moving methods require fewer grid points than adaptive static and adaptive hybrid techniques. However, adaptive moving methods are rather sensitive to the time step, non-linearity of the chemical reaction, number of grid points, and delay time for the grid motion if ignition phenomena proceed at a fast rate and/or if the steep flame front moves at a high speed. Large delay times result in grids which lag far behind the steep moving front and are not able to follow the flame.

If the number of grid points and time step used in adaptive moving methods are not sufficiently large and sufficiently small, respectively, a large number of evaluations of the Jacobian matrix is required. Furthermore, if the time step is not sufficiently small, any errors produced during ignition will affect the flame propagation at later times.

The adaptive static method required more grid points and a larger number of evaluations of the Jacobian matrix than the adaptive moving method, due to regridding and interpolation. Since the adaptive static method uses an equidistribution technique, the values of the dependent variables have to be interpolated in such a manner so as the ensure conservation and the positivity and monotonicity of the solution.

The adaptive hybrid method employed about the same number of grid points but required a larger number of evaluations of the Jacobian matrix and a smaller time step than the adaptive static technique. This is due to the uncoupling between the predictor and corrector steps, for the predictor step is used only to estimate the locations of grid points at the next time level, whereas the corrector step is used to obtain the solution in the predicted grid.

The adaptive static and adaptive hybrid methods of lines may yield oscillatory temperature profiles in front of and behind the flame front unless the time step and the number of grid points are sufficiently small and sufficiently large, respectively.

The non-adaptive methods of lines presented in this paper require a much larger number of grid points than adaptive techniques in order to resolve the flame front structure accurately and simulate fast ignition phenomena. Non-adaptive, fourth-order accurate methods of lines in space require about the same number of grid points than non-adaptive second-order accurate methods of lines in order to obtain oscillation-free temperature profiles. They also require smaller time steps if ignition phenomena proceed at a fast rate and/or if the flame speed is high, because they are based on the time linearization of the source terms and the accuracy of this linearization deteriorates as the time step is increased. Non-adaptive, operator-splitting techniques exhibit the

same characteristics as, but yield slightly slower flames than, the non-adaptive, second- and fourth-order accurate methods of lines presented in this paper.

ACKNOWLEDGEMENT

The author is grateful to Mr. Juan Falgueras of the F. Informática/E.T.S.I. Telecommunicación, Universidad de Málaga, for his TEXnical typing.

REFERENCES

1. J. I. Ramos, 'Numerical methods for one-dimensional reaction–diffusion equations arising in combustion theory', in T. C. Chawla (ed.), *Annual Review of Numerical Fluid Mechanics and Heat Transfer*, Vol. 1, Hemisphere, New York, 1987. pp. 150–261.
2. J. I. Ramos, 'Finite element methods for one-dimensional flame propagation problems', in T. J. Chung (ed.), *Numerical Modeling in Combustion*, Chapter 3, Hemisphere, New York, 1990 (in press).
3. J. G. Verwer, J. G. Blom and J. M. Sanz-Serna, 'An adaptive moving grid method for one-dimensional systems of partial differential equations', *Report NM-R8804*, Department of Numerical Mathematics, Centrum voor Wiskunde en Informatica, Amsterdam, The Netherlands, 1988.
4. J. G. Blom, J. M. Sanz-Serna and J. G. Verwer, 'On simple grid methods for one-dimensional evolutionary partial differential equations', *J. Comput. Phys.*, **74,** 191–213 (1988).
5. J. I. Ramos, 'Hermitian operator methods for reaction–diffusion equations', *Numer. Methods Partial Differential Equations*, **3,** 241 287 (1987).
6. W. J. Goedheer and J. H. H. M. Potters, 'A compact finite difference scheme on a non-equidistant mesh', *J. Comput. Phys.*, **61,** 269–279 (1985).
7. E. A. Dorfi and L. O'C. Drury, 'Simple adaptive grids for 1-D initial value problems', *J. Comput. Phys.*, **69,** 175–195 (1987).
8. L. R. Petzold, 'Observations on an adaptive moving grid method for one-dimensional systems of partial differential equations', *Appl. Numer. Math.*, **3,** 347–360 (1987).
9. S. Adjerid and J. E. Flaherty, 'A moving-mesh finite element method with local refinement for parabolic partial differential equations', *Comput. Methods Appl. Mech. Eng.*, **55,** 3–26 (1986).
10. R. M. Furzeland, J. G. Verwer and P. A. Zegeling, 'A numerical study of three moving-grid methods for one-dimensional partial differential equations which are based on the method of lines', *J. Comput. Phys.*, **89,** 349–388 (1990).
11. K. Miller, 'Moving finite elements II', *SIAM J. Numer. Anal.*, **18,** 1033–1057 (1981).
12. H. A. Dwyer and B. R. Sanders, 'Numerical modeling of unsteady flame propagation', *Report No. SAND77-8275*, Sandia National Laboratories, Livermore, California, 1977.
13. J. I. Ramos, 'Modified equation techniques for reactive–diffusive systems. Part 1. Explicit, implicit and quasilinear methods', *Comput. Methods Appl. Mech. Eng.*, **64,** 195–219 (1987).
14. J. I. Ramos, 'Modified equation techniques for reactive–diffusive systems. Part 2. Time-linearization and operator-splitting methods', *Comput. Methods Appl. Mech. Eng.*, **64,** 221–236 (1987).